Imaging the Deep Crustal Structure of Central Oklahoma using Stacking and Inversion of Local Earthquake Waveforms

Pranshu Ratre[1], **Michael Behm**[1]

[1]School of Geosciences, University of Oklahoma

Key Points:

- 3-D Pg wave velocity model for the Southern-Granite Rhyolite province in central Oklahoma up to depth of 40km.
- High velocity (Vp > 7km/s) lower crust suggests a mafic lower crust.
- High velocity anomalies observed in the upper-to-middle crust but lack of clear evidence for a rift structure related to Midcontinent rift.

Corresponding author: Pranshu Ratre, pranshu.ratre@ou.edu

Abstract

The southern Granite-Rhyolite province contains a comprehensive record of lithospheric evolution in North America. During the last decade, increased seismicity along with improved seismic monitoring installations in Oklahoma provided a rich catalog of local earthquakes. The source-receiver geometry of this dataset is well posed to illuminate the middle and lower crust through long offset recordings of the Pg phase. We present a 3-D P-wave velocity model for central and north Oklahoma developed through a non-standard processing scheme applied to local earthquake waveforms recorded from 2010-2017, focusing on the deeper crust. We employed common-mid-point sorting, stacking, and inversion of Pg-phases which resulted in a set of localized velocity-depth functions up to depths of 40 km. Using this methodology, we significantly increased the S/N ratio for far offset (~250 km) local earthquake waveforms which led to the increase in depth of investigation for our final 3-D velocity model. We find high velocity (> 7 km/s) lower crust throughout the investigated area which suggests a mafic lower crust. The high velocities support previously established models which state that the lower crust of the Granite-Rhyolite province was derived from melting of older crust. We further relate shallow and middle crustal velocity anomalies to other data sets such as gravimetric and magnetic anomalies, and the spatial distribution of earthquakes. We interpret the Nemaha Fault system as a deep-rooted discontinuity which separates two crustal domains. On the contrary, we do not find clear evidence for the existence of the Midcontinent rift (MCR) in northern Oklahoma.

Plain Language Summary

To understand how the crust in Oklahoma was created we require information from the deepest, oldest part of the crust. Waves generated by the earthquakes can be used to image the Earth's crust. The farther these waves travel, more noise is added to the data. Our technique minimizes the noise and enhances the signal observed even at stations greater than 200 km away from the earthquake source. This helps in deriving rock properties for the deepest part of the Earth's crust. Oklahoma has recently seen an exponential increase in the number of earthquakes due to oil and gas production activities. Spatially, they cover a large area in central Oklahoma, thus providing dense subsurface information in this region. We use these earthquakes and apply our technique to derive velocities of the Primary waves (P-waves) in the rocks. We observe velocity variations that indicate in-

trusive structures in the upper crust. We also observe high P-wave velocities for the lower crust which indicates that the crust is composed of high-density material. Our 3-D P-wave velocity model provides insights into the nature of the crust and also gives a deeper and more detailed picture of the regional crustal structures in Oklahoma.

1 Introduction

The study of Precambrian rocks in the midcontinent region (Figure 1) of North America is crucial in understanding the Proterozoic evolution of the North American continental lithosphere. Due to the limited exposures of the Precambrian crystalline rocks in the midcontinent region, most studies have used cores and drill cuttings to study the Precambrian geology in this region. In Oklahoma, the Precambrian basement is covered by Phanerozoic sediments except for a small area in the northeast and in the eastern Arbuckle mountains in the southeast.

Some of the early petrological and geochronological studies of the Precambrian basement rocks laid the groundwork for addressing the continental evolution in the midcontinent region (Bickford & Lewis, 1979; Bickford et al., 1981, 1986; Denison et al., 1984; Lidiak, 1996; Muehlberger et al., 1966, 1967; Nelson & DePaolo, 1985). U-Pb zircon geochronological studies from outcrop and drill cuttings established the age of these rocks to be about 1.4-1.34 Ga in the southern midcontinent (Bickford et al., 1981; Muehlberger et al., 1967). Nelson and DePaolo (1985) differentiated the rocks in the Granite-Rhyolite provinces based on Sm-Nd isotopic studies. Their "Nd-line" defines an isotopic boundary that divides the granite-rhyolite provinces based on the model ages, where rocks in the northwestern part are derived from older cratonal rocks (1.8-1.6 Ga) while rocks in the southeast of the Nd-line, from juvenile rocks (1.5-1.3 Ga) (Figure 1). Denison et al. (1984) used petrographic analysis to further divide the Precambrian basement rocks in northeastern Oklahoma. These early studies were instrumental in establishing the ages and extent of the Granite-Rhyolite province in the midcontinent but are based on outcrop and drill cuttings, and they are unable to describe the nature of the lower crustal rocks. Lack of coeval xenoliths in the midcontinent region has further contributed to our lack of knowledge of deeper crust in this region. Figure 1 shows the major tectonic provinces and crustal features in the midcontinent region.

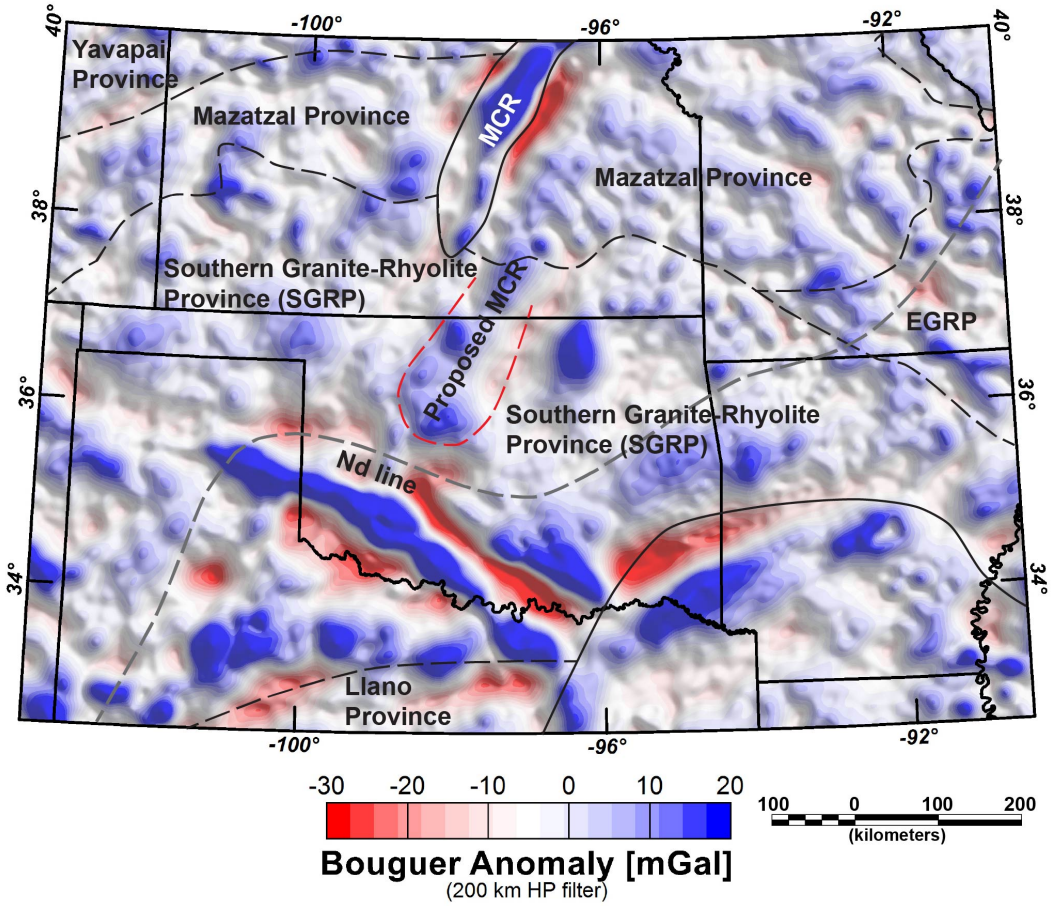

Figure 1. Tectonic provinces in the central part of the midcontinent (Modified from Bickford et al. (2015)). Bouguer gravity anomalies (based on Decade of North American Geology (DNAG) data) are shown after applying a 200 km high-pass wavelength filter to suppress upper mantle features. A possible continuation of the Midcontinent rift (MCR) in Oklahoma is shown as proposed by previous studies (see text for details). [EGRP: Eastern granite-rhyolite province].

While the earlier workers were able to establish the vast extent of this volcanic province, its origin has been debated for decades. Presence of A-type plutons further adds to the enigma of its origin (Anderson & Bender, 1989; Bickford et al., 2015; Denison et al., 1984). Based on the studies of these plutons and rocks from the granite-rhyolite provinces, several theories including extensional anorogenic settings, back-arc magmatism related to early Grenville orogeny, and back-arc and intracontinental magmatism related to accretionary tectonism in Laurentia of 1.6-1.3 Ga, have been considered (Amato et al., 2011; Anderson & Bender, 1989; Whitmeyer & Karlstrom, 2007). Recent Lu-Hf studies by Bickford et al. (2015), provide a new model for the formation of the granite-rhyolite

province of the midcontinent. Their isotope data corroborates the presence of Nd-line as given by Nelson and DePaolo (1985). They suggest basaltic underplating as part of the mechanism that led to the melting of lower crustal rocks that intruded to form the granite-rhyolite provinces. Evidence for basaltic underplating can be interpreted as high velocity (P-wave velocity 6.9-7.5 km/s) lower crustal layer, as observed for e.g. by Karlstrom et al. (2005) and Thybo and Artemieva (2013) through deep crustal seismic velocity models in other parts of the world. However, such deep crustal seismic studies with sufficient vertical and horizontal resolution are scarce for the Granite-Rhyolite province.

Another intriguing feature in the midcontinent is the ~3000 km long Midcontinent rift (MCR), a failed rift that formed ca. 1.1 Ga within Laurentia (Hinze et al., 1997; Van Schmus & Hinze, 1985). During the 20-40 Myr rifting event, vast amounts of igneous rocks followed by sedimentary rocks were deposited within the rift. The signatures of Midcontinent rift are observed as high gravity anomalies stretching from the Great Lakes to central Kansas (Hinze et al., 1997; Sims et al., 2005; Van Schmus & Hinze, 1985). Several authors extend the MCR into north central Oklahoma based on relatively high gravity anomalies that appear to continue from the gravity anomalies observed in the north (Kolawole et al., 2020; C. A. Stein et al., 2014, 2015) (Figure 1). Unlike modern rifts where decreased crustal thickness due to extension is observed (Thybo & Artemieva, 2013), crustal thickening is observed for the northern part of the MCR (Chichester et al., 2018; Hinze et al., 1997; Shen et al., 2013; Zhang et al., 2016). Increased crustal thickness is attributed to a compressive event that inverted the rift, after it had already failed (C. A. Stein et al., 2015, 2018). Studies by Chichester et al. (2018) and Zhang et al. (2016) were conducted in the northern, more prominent part of the MCR. There is evidence for underplating beneath the MCR in certain regions (Chichester et al., 2018; Woelk & Hinze, 1991; Zhang et al., 2016). Surface evidence for the rift is not observed in Oklahoma, and so deep crustal studies that reveal the seismic structure can inform about the presence or absence of the rift feature in Oklahoma.

Despite emphasis on seismic studies for hydrocarbon exploration in its sedimentary basins, Oklahoma is significantly under-explored by means of deep crustal-scale seismic imaging campaigns. Consequently, knowledge of the deep crustal structure is limited and constrained to a few locations only. The recent increase in induced seismicity due to oil and gas production (Ellsworth, 2013; Keranen et al., 2014) and the subsequent efforts in instrumentation to monitor this activity, which also coincided with the ongoing de-

ployment of US transportable array across United States, resulted in a large-scale passive seismic experiment, albeit unintentional. We make use of local earthquake data recorded across 10 networks between 2010-2017 to develop a 3-D P-wave velocity model of the crust for central Oklahoma, a core part of the Precambrian midcontinent crust. As the station coverage and earthquake distribution resembles an irregular 3-D active seismic experiment, we employ active seismic processing techniques of common mid-point sorting and stacking to the local earthquake waveforms. This improves the signal-to-noise ratio and simplifies the wavefields of the recorded data, allowing for imaging of deeper structures and large areas. Our study aims to contribute to understanding the evolution of this understudied part of the midcontinent crust. Furthermore, we suggest a workflow for processing local earthquake data which is potentially applicable to other areas as well. In this paper we present and discuss our methodology and geologic and tectonic implications from our derived 3-D seismic model.

2 Regional Geology and Previous Geophysical Studies

2.1 Geology

The evolution of Laurentia through a periodic and continued accretion of igneous material via volcanic and island arcs over the Archean cratons is the most widely accepted model of the formation of lithosphere in the continental United States (Whitmeyer & Karlstrom, 2007). The Mazatzal Orogeny ca. 1.65-1.6 Ga resulted in the accretion of juvenile volcanic arcs forming the older crustal rocks in Oklahoma (Whitmeyer & Karlstrom, 2007). Although the southern extent of the Mazatzal province has not been mapped, isotopic evidence by Nelson and DePaolo (1985) and core and outcrop evidence from surrounding states of New Mexico and Kansas suggest an extension of this province beneath the Granite-Rhyolite province of Oklahoma (Anderson & Bender, 1989; Whitmeyer & Karlstrom, 2007).

The Mazatzal orogeny was followed by the accretion of the Southern Granite-Rhyolite province (SGRP) ca. 1.5-1.35 Ga. The Sm-Nd isotopic study by Nelson and DePaolo (1985) provided a major breakthrough in understanding the origins of SGRP. Their studies lead to the conclusion that these rocks were derived from older crustal rocks. This study was further supported by Van Schmus et al. (1996) who calculated Sm-Nd model ages showing the Mesoproterozoic rocks of SGRP with a consistent increase in age mov-

ing from southeast to northwest. The tectonic setting of the SGRP and the coeval A-type plutons have been studied and evaluated by various workers. Whitmeyer and Karlstrom (2007) suggest a convergent and transpressional setting wherein the emplacement of Granite-Rhyolite province was caused by a tectonic episode away from the plate margins. Amato et al. (2011) suggest an extensional or transpressive setting for the Granite-Rhyolite terrain based on their studies of granitic plutons in Burro Mountain, New Mexico, which are coeval with the basement rocks of Oklahoma. Studies based on A-type plutons indicate an anorogenic origin, suggesting the source of these plutons as partial melting of juvenile crust (Anderson & Bender, 1989). A recent study by Bickford et al. (2015), presents new geochronological and isotopic data for samples across the mid-continent region of United States. Their zircon age studies revealed that the continental scale magmatism was long lived (150-200 Ma) and locally episodic as given by the bimodal zircon age distribution in the midcontinent (Bickford et al., 2015). Lack of zircon in many samples analyzed by Bickford et al. (2015), along with magma temperatures derived from the existing zircon samples suggest temperatures above 850 °C. Their conclusions are similar to study by Goodge and Vervoort (2006), who analyzed Hf isotope compositions in the zircons in samples from Penokean (1.9-1.8 Ga), Mojave (1.8-1.7 Ga), Yavapai (1.8-1.7 Ga), and Granite-Rhyolite (1.5-1.3 Ga) provinces. Studies of A-type plutons also suggest their formation from partial melting of tholeiitic magma (Frost & Frost, 2011, 2013; Shaw et al., 2005). Bickford et al. (2015) suggest a convergent plate boundary model at the northeastern margins of Laurentia that led to creation of back arcs in the continental interior. They argue that the convergent active margin can lead to destabilization of the back arcs. This can cause delamination of the lithosphere, consequently leading to a shallower lithosphere-asthenosphere boundary and higher temperatues at shallower depths which may induce crustal melting. This model seems to agree with the models suggested by Karlstrom et al. (2001), Slagstad et al. (2009), and Whitmeyer and Karlstrom (2007).

The Precambrian accretion of the crust was followed by opening of the Iapetus Ocean in late-Neoproterozoic - early-Cambrian and the formation of the Southern Oklahoma Aulacogen (SOA) (Gilbert et al., 1993; Buckey, 2012; Thomas, 1991; Whitmeyer & Karlstrom, 2007). SOA comprises of the Wichita uplift, the Arbuckle uplift and the Anadarko basin. The evolution of these structures continued through the Cambrian through, continued subsidence, deposition, erosion, and intrusion of igneous rocks (Keller et al., 1983). Finally, intense deformation and erosion during the Pennsylvanian associated with the An-

cestral Rockies orogeny led to the present-day configuration of the tectonic features, including the Nemaha Uplift, we observe today in Oklahoma (Figure 2) (Garner & Turcotte, 1984; Gilbert et al., 1993; Johnson, 2008).

Gravity and magnetic data can provide some information on the crust (Bickford et al., 1986; Van Schmus et al., 1996; Sims et al., 2005), but non-uniqueness of these methods require constraints such as seismic data to infer robust interpretations. The lack of rock samples from deeper crust in Oklahoma further limits our understanding of this part of the crust.

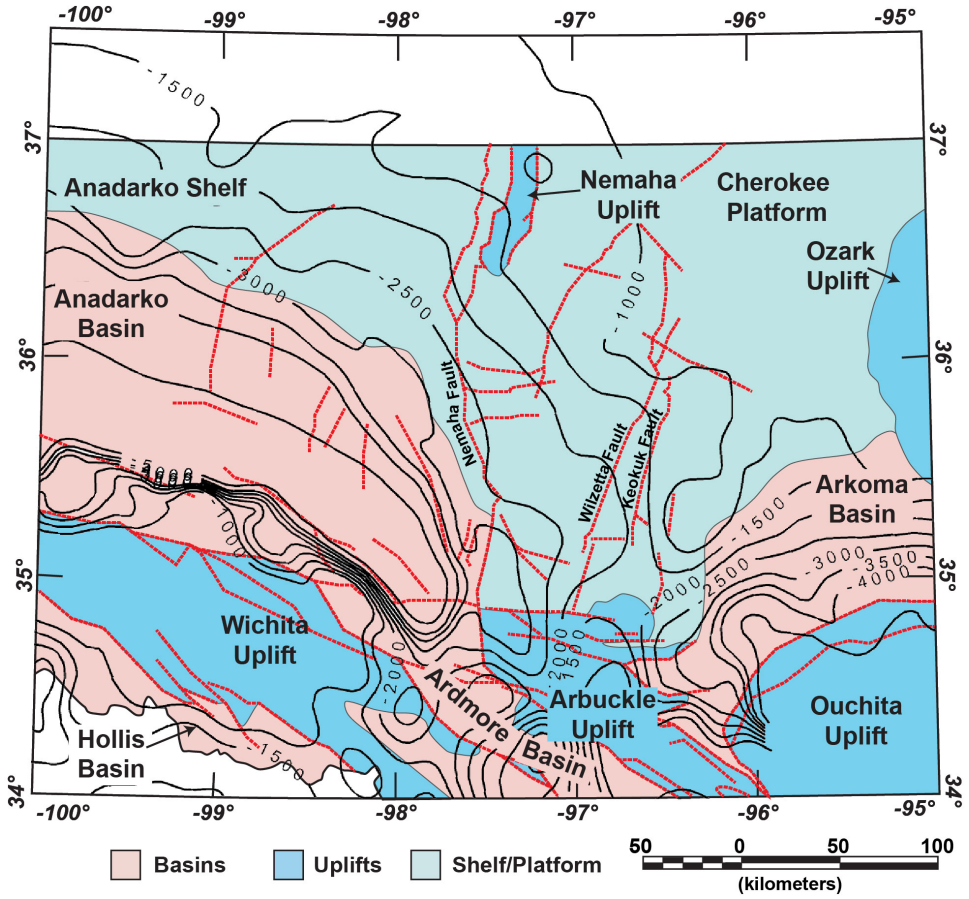

Figure 2. Major tectonic features in Oklahoma (adapted from Northcutt and Campbell (1996)). Red dashed lines: major fault systems. Black solid lines: depth-to-basement contours (meters) computed from basement well information as given by (Campbell & Weber, 2006).

187 ### 2.2 Previous Seismic Studies

188 Tryggvason and Qualls (1967) derived a simple layered model for Oklahoma's crust
189 through a 2-D active seismic refraction study. The ~450 km profile runs northeast-southwest
190 across Oklahoma, cutting through different tectonic units (Figure 3). Based on recordings
191 of multiple shots at 2 shot points in Chelsea, NE Oklahoma, and Manitou, SW Oklahoma,
192 at 26 seismometers between the shot points, they interpreted a homogeneous three-layer
193 earth model and provided the first look at the depth of Moho and crustal velocity varia-
194 tions in Oklahoma. The same 2D line was re-processed and integrated with other datasets
195 by Mitchell and Landisman (1970) who derived a more detailed crustal model. They used
196 seismic refraction and reflections observed from the Tryggvason and Qualls (1967) - 2D
197 profile, gravity anomaly data, basement depth data, and well-log data. Their final veloc-
198 ity model showed homogeneous crustal layers below the upper crust (up to 18 km). They
199 modelled the shallow upper crust in much greater detail as compared to the earlier model
200 and observed discontinuities due to the presence of fault zones cutting through the profile.
201 They interpret the crustal thickness to be between 46 - 46.5 km with P- wave velocities up
202 to 7.39 km/s for the lower crust.

203 In the late 1970s, deep seismic reflection profiles were shot by Consortium for Con-
204 tinental Reflection Profiling (COCORP) and a 2-D wide angle reflection/refraction sur-
205 vey by University of Texas at El-Paso (UTEP) and University of Texas at Dallas (UTD)
206 in 1985. Both of these surveys aimed to understand the deeper structure of Wichita Up-
207 lift and characterize structural features at the boundary of Southern Oklahoma Aulacogen
208 and the Anadarko Basin. Several authors worked on developing a 2D velocity structure
209 across Wichita uplift and Anadarko basin using this data (e.g. Agena et al., 1989; Brewer
210 et al., 1983, 1984; Brewer & Oliver, 1980; Phinney & Jurdy, 1979; Zhu & McMechan,
211 1989, and others.). These investigations revealed a layered basement about 12 km thick
212 and a thick crust with depth to Moho varying from 40-45 km (Lynn et al., 1981; Pratt et
213 al., 1992). The UTEP-UTD seismic survey was reanalyzed by Buckey (2012), who was
214 able to identify more reflections. The author further used gravity data to obtain a detailed
215 velocity and geologic model for the upper – mid crust up to 20 km depth. They report
216 a deeper Precambrian basement as compared to Pratt et al. (1992), overlain by metased-
217 iments, rift fill and Proterozoic basin fill. Figure 3 shows locations of the various active
218 seismic surveys conducted in Oklahoma.

There have been a few passive seismic studies targeting large scale crustal structure in Oklahoma. Local earthquake tomography by Chen (2016) and Toth (2014) obtained upper crustal (up to 15-20 km) seismic velocity. Velocity anomalies observed in these models show close correlation to the major tectonic features like the Nemaha Fault Zone and the Wilzetta Fault Zone in Oklahoma. A high resolution but shallow anisotropic Pg velocity was developed for central Oklahoma by Pei et al. (2018). It shows lateral velocity variations in the uppermost crust (5-10 km). Receiver function analysis and Pn tomography by Tave (2013) using the data from US transportable array network revealed deeper discontinuities like Moho and Hales discontinuity. The author presents depths to the Moho between 36 km and 42 km throughout the state. McGlannan and Gilbert (2016) reported a crustal depth variation from 30-55 km across the state of Oklahoma, which they calculated from the Earthscope Automated Receiver Survey using the US transportable array. In general, the passive seismic studies conducted in Oklahoma so far either do not have the necessary depth of investigation to image the deeper crustal structures (Chen, 2016; Toth, 2014), or lack the resolution required to be able to comment on the regional crustal structure (Evanzia et al., 2014; McGlannan & Gilbert, 2016). Our methodology aims to address these problems and obtain a deeper seismic model that can highlight the regional crustal features in Oklahoma.

3 Data and Methodology

Local earthquakes are commonly used for imaging in seismically active regions. Local earthquake tomography (LET) uses travel times of earthquake phases to invert for the velocity structure, while often simultaneously (re-)locating the earthquake source (e.g. Kissling et al., 1994; Rawlinson & Sambridge, 2003). The term 'local' refers to a spatial overlap between sources and receivers, e.g. the receiver array should enable the recording of crossing rays at all incidence angles, and therefore allow for a tomographic inversion for both velocity structure and hypocenters.

Earthquake depths play a crucial role for the depth of investigation in LET. For a given velocity gradient, waves from shallow earthquakes recorded at large offsets reveal information from the deeper crust, while deep earthquakes record deep crustal information at short offsets due to their sub-vertical ray paths (Braeuer et al., 2012; Tong et al., 2017). The signal-to-noise (S/N) ratio also decreases with offset (source-receiver-distance) for both shallow and deep local earthquakes, which ultimately leads to a lower depth of in-

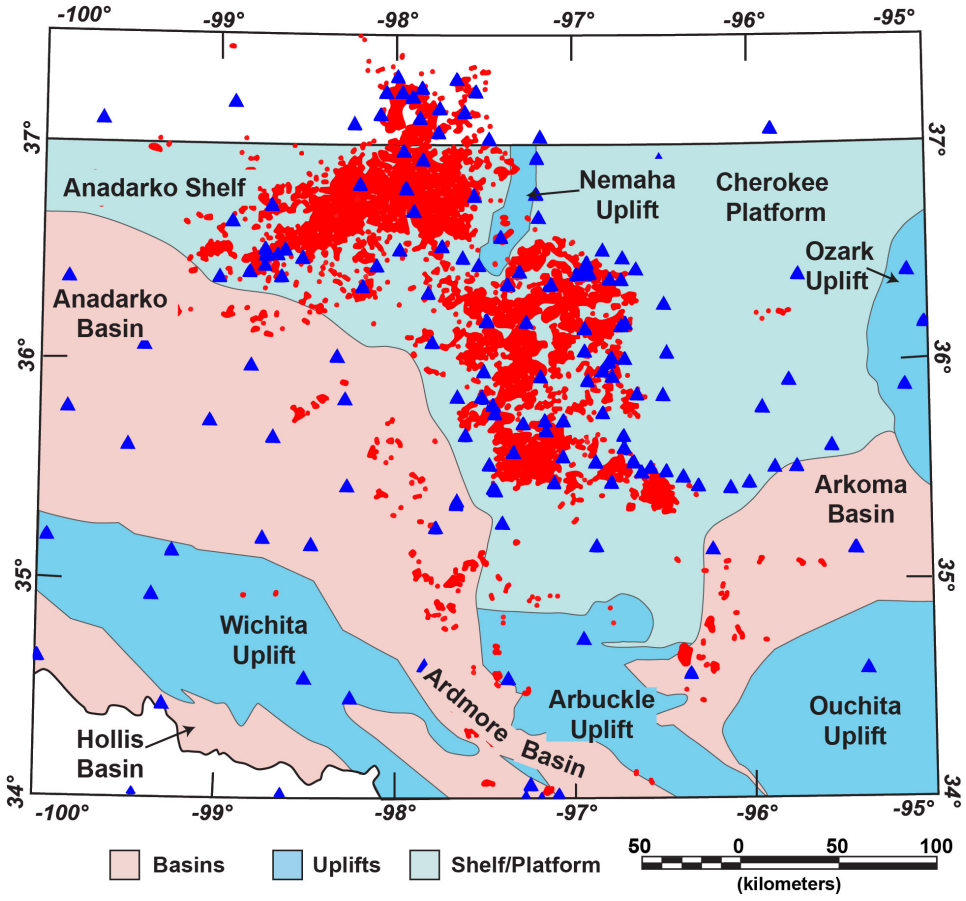

Figure 3. Black thick lines: previous active seismic studies conducted in Oklahoma for crustal investigations. Red dots: location of earthquakes used in this study. Blue triangles: stations used in this study.

vestigation when using shallow earthquakes only. The traditional LET approach involves identifying and picking seismic phases across different stations. Sparse distribution of recording stations is common in passive seismic network geometries and makes correct phase correlation and identification difficult. Estimating robust travel times at large offsets is challenging, in particular for small magnitude events. Consequently, traditional LET methods in Oklahoma where the earthquake depths are shallow (~2-7 km depth) (Figure S1) can only represent velocity variations in the upper crust (Chen, 2016; Toth, 2014). Interpretation of individual travel times requires data of high quality, and in the case of many observations, (semi-)automated phase correlation and picking routines (Chen, 2016; Thybo et al., 2006).

To overcome the issues of low S/N ratio and ambiguous phase correlations, we propose to stack waveforms and apply specifically designed processing and inversion rou-

tines. This approach has been successfully applied to active source 3-D wide-angle refraction/reflection (WAR/R) data as well as earthquake sources to both P- and S-wavefields (Behm, 2009; Behm et al., 2007; Buehler & Shearer, 2013; Loidl et al., 2014). We use existing localizations of the events (Schoenball & Ellsworth, 2017) and consider the data set as an active 3-D acquisition with irregular geometry. Using the principle of reciprocity, the small number of recording stations is compensated by a large number of events. We aim for stacking and inversion of Pg (refractions from the crust) phases to derive a 3-D P-wave velocity model of the crust. Stacking is preceded by sorting to common-mid-point (CMP) gathers, as wide-angle refractions best approximate the seismic structure at the common-midpoint location where the ray travels horizontal. Pre-stack processing aim at enhancing and simplifying the wavelets such that the under-sampled wavefields can stack constructively. Stacking has a tendency to favor robust models, that is relative insensitivity to randomly distributed data outliers (Behm et al., 2007). CMP regionalization leads to a set of local 1-D travel time curves approximating the crustal structure at the CMP location. Those travel time curves are picked and inverted, and the derived set of local 1-D velocity models is eventually combined into a smooth 3-D Pg velocity field.

3.1 Data

We use 27,568 local earthquakes recorded at 165 broadband stations belonging to 6 different networks across Oklahoma (Figure 3). The earthquake events were recorded between the time period January 2010 to September 2017. We use a catalogue which combines relocation from Schoenball and Ellsworth (2017) and HypoDD corrected catalogue. Hypocenter solutions (including origin time) in those catalogs are associated with uncertainties, which will be addressed in section 3.2.4. Earthquake depths vary from 2-7 km and we select the maximum epicentral distance for P-wave velocity evaluation to be 250 km. Finally, we have 1,214,112 individual seismic traces that we use for further processing. Station information and earthquake events used are provided in data set S1 and S2.

3.2 Pg Processing

The workflow to derive a 3-D crustal P-wave velocity from the Pg phase comprises six steps:

1. Geometric and kinematic corrections to account for varying source depths and sedimentary thickness at the receiver locations.
2. Pre-stack signal processing to increase the S/N ratio and to facilitate constructive interference.
3. CMP sorting and stacking in offset bins to derive local 1-D travel time curves.
4. Manual picking of the 1-D travel time curves.
5. Inversion of 1-D picked travel time curves for local 1-D velocity-depth functions representing the CMP location.
6. Combination of all 1-D velocity models into a 3-D velocity model.

3.2.1 Geometric and Kinematic Corrections (Datuming)

Time and geometric corrections are required to account for the different earthquake depths and sedimentary thickness at the receiver locations. First, to correct for the elevation difference between source and receiver of each earthquake-receiver pair, we choose the corresponding earthquake depth as datum and apply time and offset corrections to shift the receiver to this datum. Second, stacking of different source-receiver pairs requires all data to be at the same reference level. We choose a depth of 5 km as our final datum since most of the earthquakes in Oklahoma are within ~5-7 km depth range (Figure S1). This introduces further time corrections and offset shifts for both the source and receiver locations.

Datum corrections for wide-angle refractions depend on the earthquake depth, source-receiver offset, basement structure at source and receiver, and the regional velocity structure. As opposed to simple static corrections for steep-angle reflections, the combined effects of velocity structure, basin geometry and velocities, and offset dependency introduce a high degree of nonlinearity. Calculation of exact time and geometric corrections would require a 3-D velocity model of the crust, which we do not have at this stage. As an approximation for the purpose of those corrections, we use a 1-D velocity model for the crust below basement based on the Christensen and Mooney (1995) model for continental shields. A 1-D velocity model for the sedimentary cover above basement is taken from the OGS velocity model for Oklahoma (Darold et al., 2015). An extrapolated basement depth map calculated from basement penetrating wells and regional gravity data (Campbell, 2007) is used to derive the basement depths at each source and receiver location. We cal-

culate offset-dependent time and offset corrections for a range of earthquake depths and receiver basement-depths using the raytracing code ANRAY (Gajewski & Pšenčik, 1987; Gajewski & Pšenčík, 1989). Finally, those corrections are interpolated for the actual earthquake and receiver locations for each source-receiver pair. The corrections are largest for shallow offsets and deep earthquakes (Figure S2).

3.2.2 Pre-stack Signal Processing

We apply a minimum phase Ormsby bandpass filter with corner frequencies of 2-4-6-8 Hz to increase the S/N ratio. To facilitate constructive interference of the Pg phase, we convert the data to their envelope (modulus of the complex trace). Bandpass filtering and envelope calculation also lifts the requirement of instrument response removal. This step is crucial since the receiver spacing is large, and wavelets from different events cannot be expected to be in phase after CMP sorting. We further increase the visibility of the Pg phases, in particular at larger offsets, by applying the STA (short-term average) to LTA (long-term average) ratio signal detection algorithm (Astiz et al., 1996). The averaging windows used for STA and LTA are 0.1 s and 10 s respectively and have been decided after testing. Figure 4 shows the result of pre-stack signal processing on one event gather.

3.2.3 CMP Sorting and Stacking

The signal-processed traces are sorted into common mid-point (CMP)-gathers and stacked in offset bins. The study area is divided into cells such that the traces whose CMPs fall into a particular defined cell are sorted into one gather. The offset-sorted Pg phases in this gather represent travel time curve for the velocity-depth function at the cell location (Behm et al., 2007). Rectangular cells are centered on a regular grid with 10 km lateral spacing, and the cell size is automatically varied between 10-70 km throughout the study area depending on the number of traces which fall into each gather. The variable cell size accounts for the irregular geometry and is smallest in the central part of the study area (Figure 5). The final location of the cell is calculated as the average location of all the trace CMPs in the gather, and the cell size represents the average distance of all trace CMPs to the final cell location.

In each CMP gather, the traces are subjected to a linear move-out (LMO) correction with a velocity of 6 km/s and finally are stacked in 5 km offset bins. The absolute offset

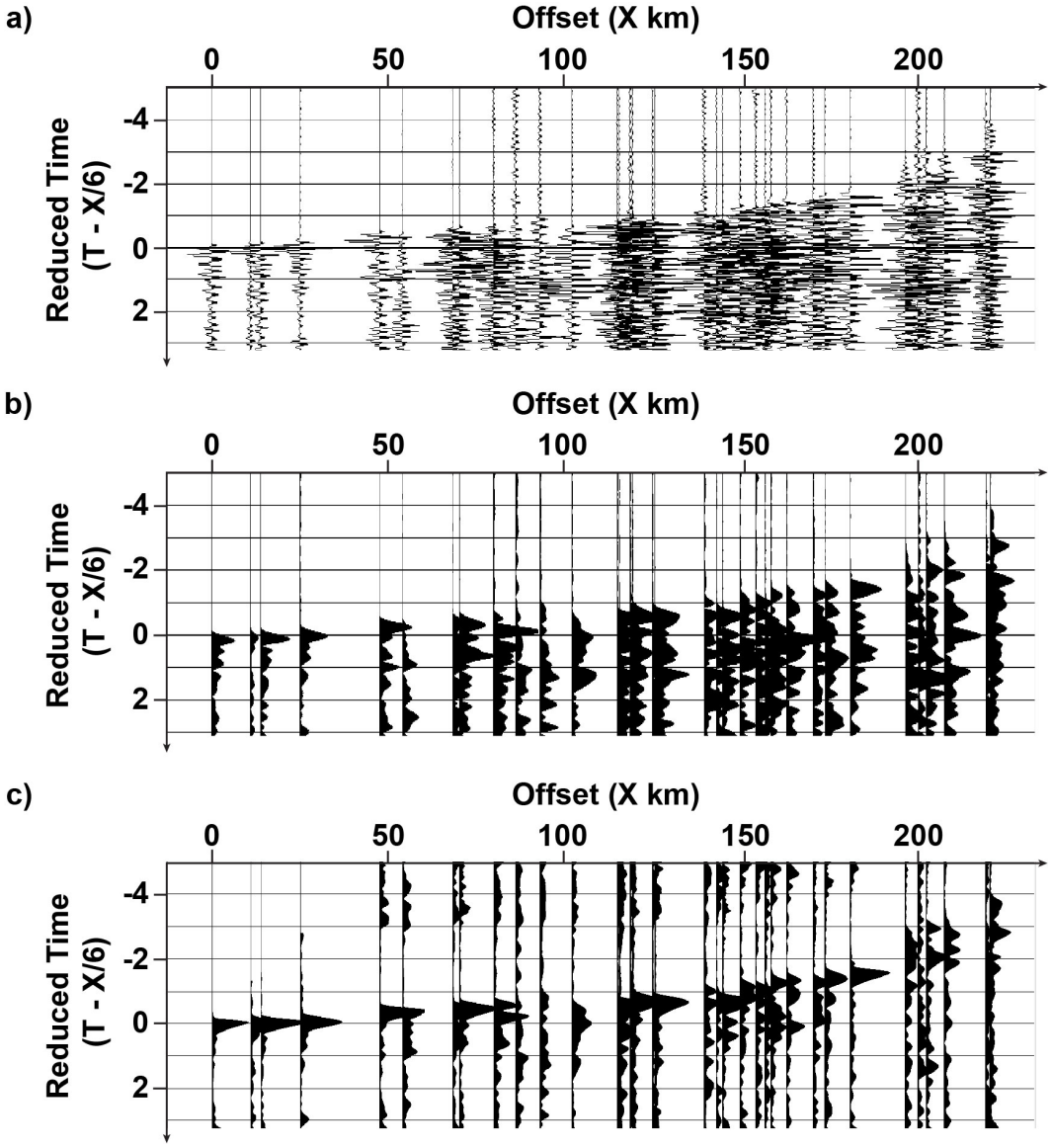

Figure 4. Example of preprocessing on one datum-corrected event gather with a linear move-out for a velocity of 6 km/s. a) bandpass filtered (2-4-6-8 Hz), b) signal converted to envelope, c) STA/LTA applied.

of each stacked trace is calculated as an average of all traces in the bin. The stacked CMP gathers allow for a first qualitative assessment of the influence of the source depths, and the errors in event location and origin time as reported in the catalogue. Prior to sorting and stacking, we calculate a relative quality value for each event which depends on source depth and the hypocenter errors in both depth and lateral position. A large quality value is obtained for shallow earthquakes and small errors, and the events are sorted by descending quality value. Sorting and stacking are performed on (1) the first 10% of the events (high-

quality data only), (2) the first 50% of the events (high to medium quality data), and (3) to all events (high to low quality data). Figure 6 shows the trade-off between using a small number of high-quality events vs. including a larger number of low-quality events. E.g. non-physical humps in the travel time curve and overall low S/N ratio are more effectively mitigated in the 50% dataset, which includes earthquakes in the depth range 5 to 7 km. Consequently, we chose this data subset for further processing.

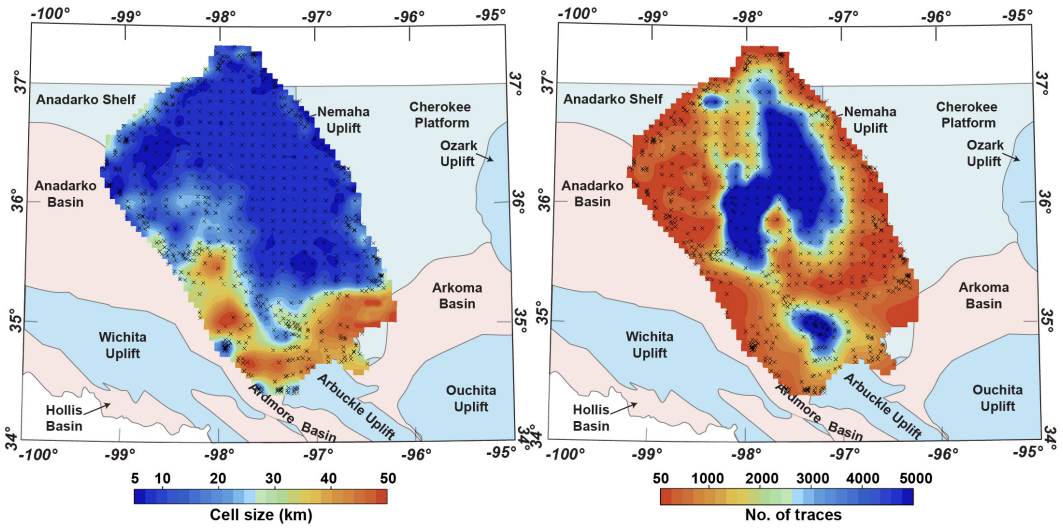

Figure 5. (a) size of the CMP bin, (b) number of traces in each CMP bin. CMP bin center locations are shown as "x".

3.2.4 Travel Time Curve Picking

In traditional local earthquake tomography (LET), accurate travel time picks provide the arrival times for seismic phases which are then inverted to determine the subsurface velocity structure. In contrast, we are picking 1-D travel time curves instead of arrivals on individual traces. Before picking is performed all stacked gathers are bandpass filtered with a 0.04-0.08-0.5-0.8 Hz Ormsby filter. The stacked gathers have high S/N ratios but due to the process of envelope calculation, stacking and low-pass filtering, the phase of the waveform is lost. To ensure consistency, we pick smooth arrival time curves along the maximum amplitude of the stacked traces. On average, the maximum of the filtered envelope wavelet corresponds to a theoretical travel-time curve based on a 1-D velocity model for continental shields (Christensen & Mooney, 1995). 1-D travel time curves have to represent a layer-cake earth model, and as such are more constrained than 3-D travel time

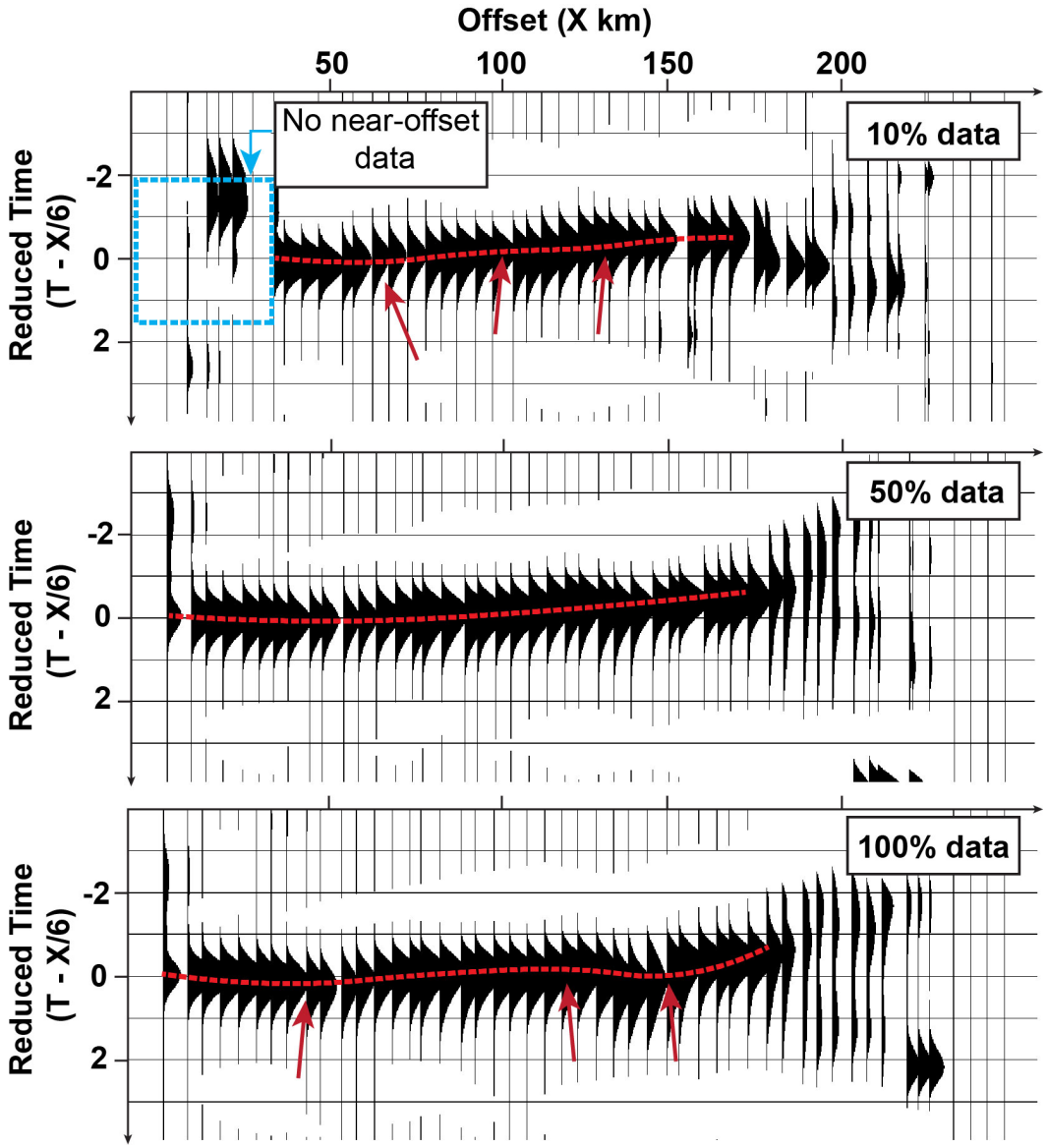

Figure 6. Comparing the stacks for 10%, 50%, and 100% data sets (see text for details). Red arrows indicate the unrealistic deviations in the travel time curve for 10% and 100% data sets.

curves. This implies that humps or similar (e.g. non-smooth) irregularities in the travel time curve should not be picked. Such deviations from a smooth curve may be caused by localized gross errors in hypocenter and/or origin time solutions, and we avoid picking such arrivals (Figure 7). Continuity and smoothness of the travel-time curve is a requirement for the assumption of a layer-cake earth model, and introduction of humps in the curve will not be representative of geologic structures. A problem resulting from the sparse station distribution is a general lack of representative near-offset traces due to the

depth of the sources. We only picked smooth travel time curves on stacked gathers where enough near-offset traces were available for a stable inversion. Examples for some of the stacks and corresponding time-picks are shown in Figure 7. Finally, we manually inspect our picks for lateral consistency across the CMP gathers and picks are removed and/or corrected if required. We finally obtain 1-D travel time curves representing the velocity-depth function at each CMP location.

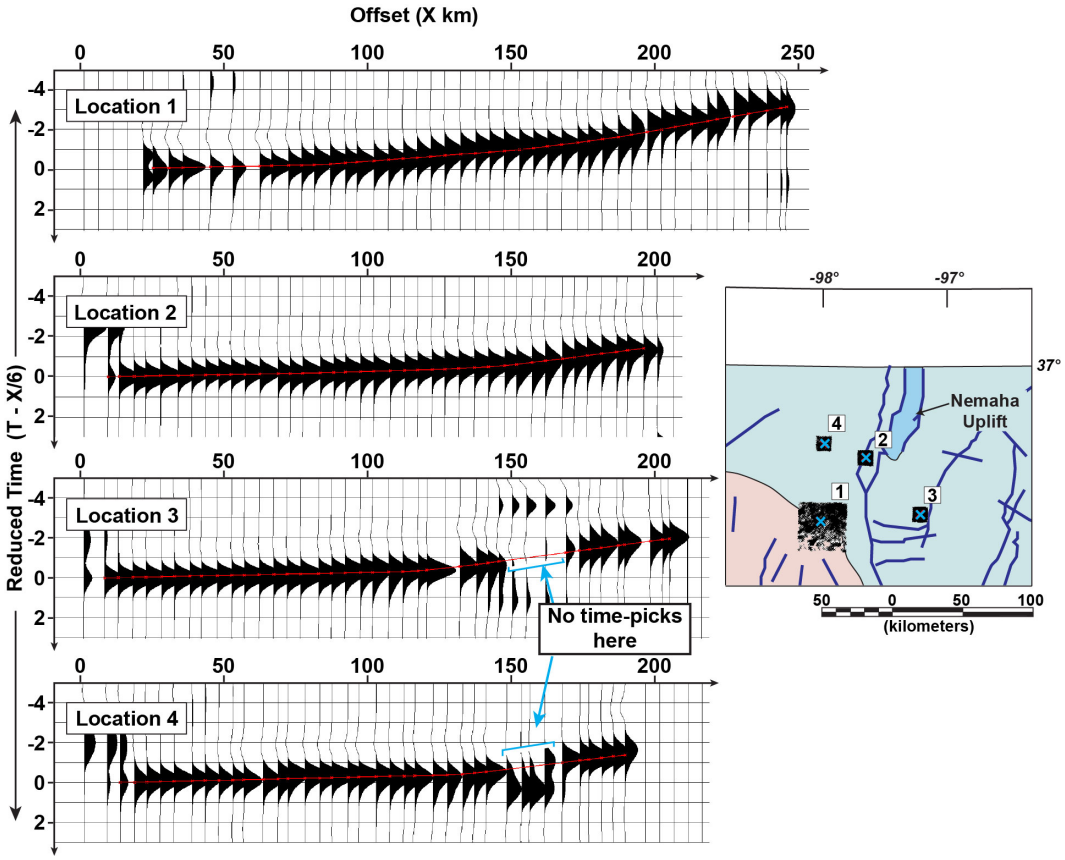

Figure 7. Examples of stacks from different locations. The map on the right shows the location and size of CMP bin for each of the stacked gathers. Note the larger CMP bin size for location 1. Small black cross:location of individual CMPs (for each source-receiver pair) within one CMP bin. Blue cross: CMP bin center locations.

3.2.5 1-D Travel Time Inversion and Combination into a 3-D Model

The 1-D travel time curve at each CMP location represents a 1-D velocity-depth function at that location. Assuming an initial 1-D velocity model for the crust, the 1-D travel time curves are inverted to obtain the velocity information using a ray parameter

weighted scheme (Behm et al., 2007). Our initial velocity model is derived from the local Oklahoma velocity models for the sedimentary layer (Darold et al., 2015) and the shields and platforms velocity model as given by (Christensen & Mooney, 1995) for the basement and below. The inversion provides a 1-D velocity-depth function at each location along with corresponding resolution elements as the output. The resolution elements define the confidence on each of the final computed velocity elements. We also test the robustness of our final velocity model based on different initial velocity models (Figure S3). The entire workflow (CMP sorting, stacking and travel time picking, inversion) is illustrated in Figure 8.

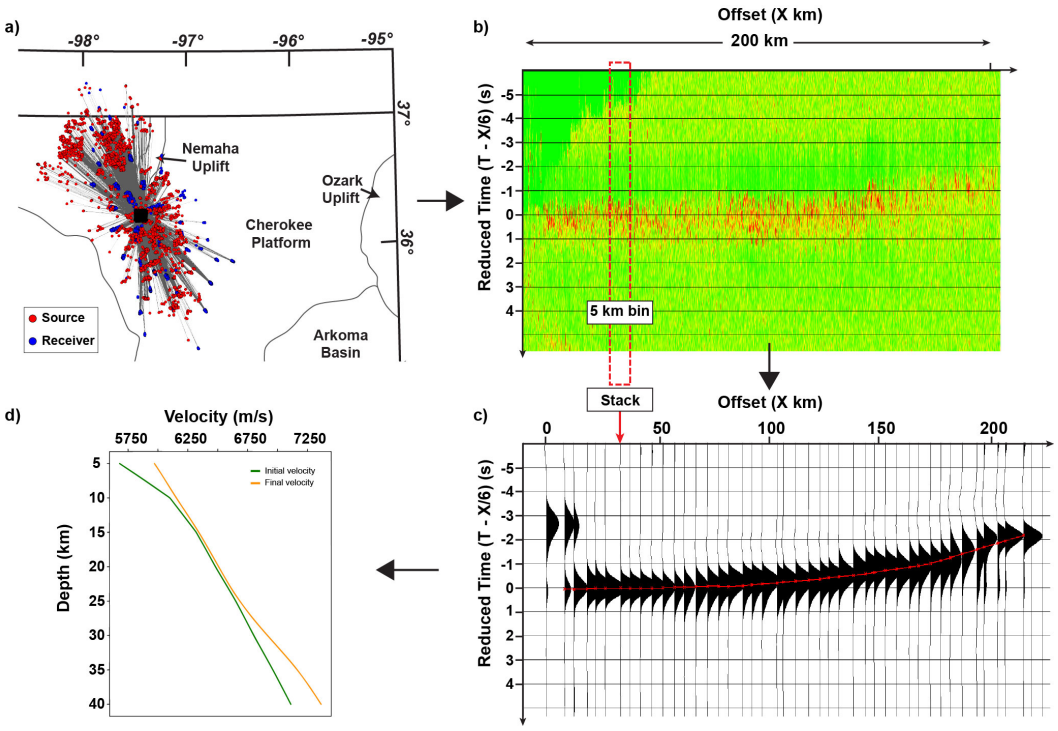

Figure 8. Processing steps illustrated for one CMP bin. (a) All source-receiver pairs (grey lines) shown for the CMP bin (black square); (b) Pre-processes earthquake waveforms in this CMP bin arranged according to their offsets with a linear move-out correction of 6 km/s; (c) Stacked gather obtained from 5 km offset-bin stacking of sorted gather in b), red dashed line shows the picked travel time curve; (d) Initial and inverted 1-D velocity model obtained for the CMP bin location.

We finally combine the 1-D velocity models derived at each of the CMP locations into a 3-D velocity model based on kriging interpolation approach. We present a 3-D velocity model for Oklahoma that captures regional crustal structures up to depths of ~40

km. Average velocities vary from 5.96 km/s at 5 km depth to 7.24 km/s at 40 km with an overall minimum and maximum of 5.56 km/s and 7.39 km/s respectively. Average velocities for upper-to-middle crust (10-25 km) are very similar to the 1-D global velocity model as given by Christensen and Mooney (1995) for shields and platform. We observe higher average velocities for the uppermost crust (5-10 km) and the lower crust (>25 km). Figure 9 shows combined velocity model as depth slices at 5 km interval starting from 5 km to 40 km. Our velocity model starts at 5 km depth, where we have assumed our processing datum. Due to velocity increase with depth, we chose a depth-dependent color scale in Figure 9 to emphasize lateral variations at each depth. To analyze the velocity model in more detail we have highlighted regions (Figure 9, Regions A, B, C) which show velocity anomalies which are discussed in more detail in section 4.

4 Discussion

4.1 Comparison with Existing Velocity Models

There have been two major studies that have developed regional velocity models for the crust in Oklahoma. Chen (2016) developed a 3-D velocity model for the upper crust (up to ~15 km depth) using traditional travel time tomography applied to local earthquake waveforms. We are able to co-locate the velocity anomalies mentioned in regions A, B, and C to the similar velocity anomalies observed in the cross-sections A4 and A5 (Figure S4) from Chen (2016)'s model. They interpret the high velocity anomalies of region A as the Midcontinent Rift and regions B and C as intrusions in the crust. The depth of investigation for their model is limited to about 15 km.

The second regional velocity model was developed by Pei et al. (2018) who used a 2-D lateral tomographic technique (Pei et al., 2013) to obtain a high-resolution anisotropic velocity for the uppermost crust. Their model represents depth-averaged velocities model for the 5-10 km in the upper crust based on travel times with offsets up to 130 km. We observe significant differences in some areas when comparing our results to this model. High velocity anomaly in region A (Figure 9) is not observed in their model, but they model a very high velocity anomaly just south-east of region A. They also observe less prominent high velocity anomalies west of region A (Figure 9) high velocity anomaly. These differences might be related to the different methodologies used in calculating the velocity models. Pei et al. (2018) chose a data set with epicentral distances varying from

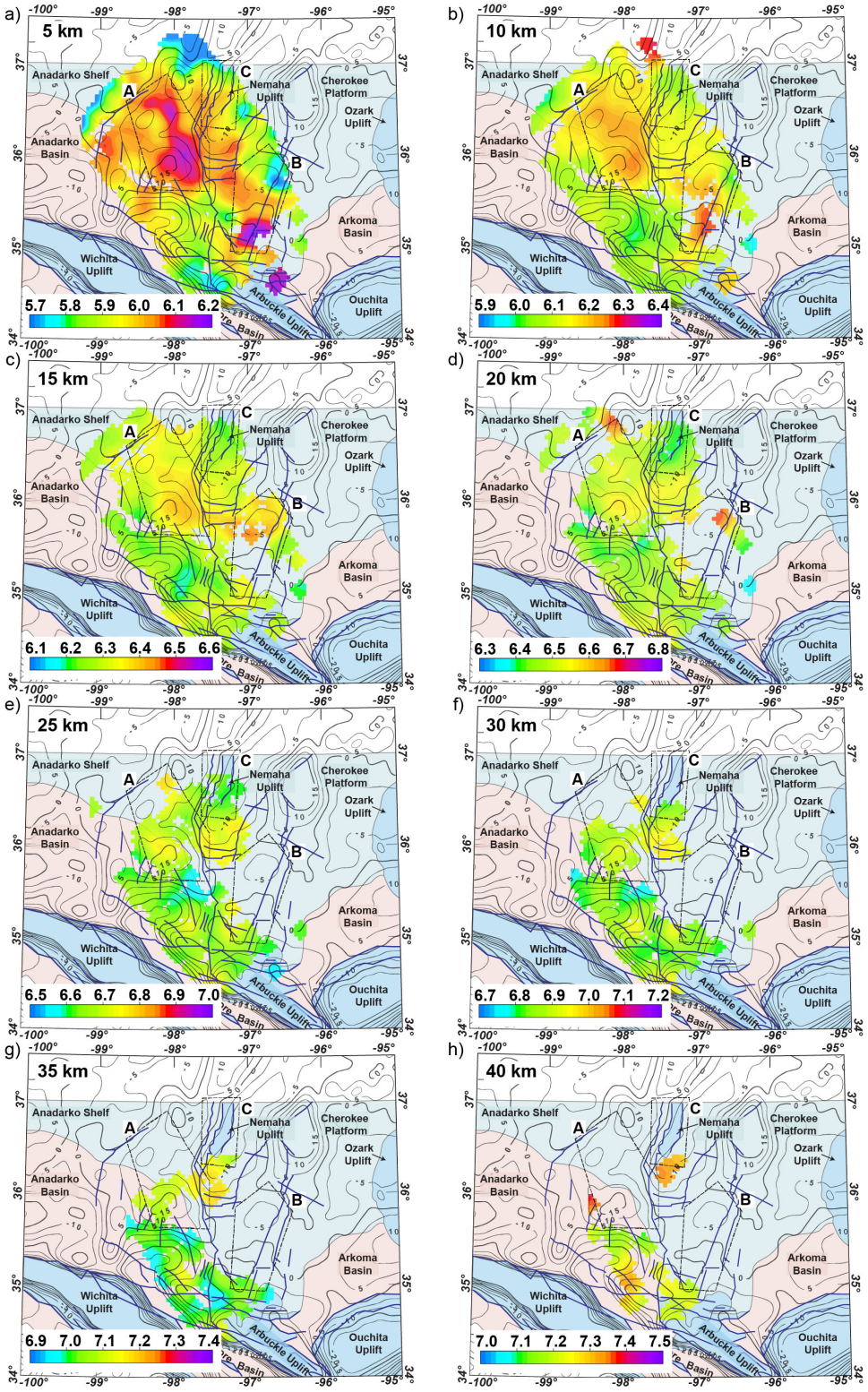

Figure 9. Horizontal slices through the 3-D Pg wave velocity model. Note the varying color scale for each depth slice (same range of 500 m/s).

~32 km to ~130 km and assumes a head wave ray path for all the travel times irrespective of the epicentral distance. As the Pg phase dives down with increasing offset, the head wave path assumption for offsets as far as 130 km can introduce variations in the final velocity model which may lead to artifacts in velocity imaging. Our calculations show that the curved ray paths at 120 km offset penetrates down to 15 km depth (Figure S5). Assuming a head wave geometry, the velocities in the mid-crustal depth range between the hypocenters and 15 km will be projected to the shallow part of the basement. Another point of difference is the model assumption of isotropic crust in our model whereas Pei et al. (2018) considers anisotropy.

4.2 Crustal Structures

The upper crust in Oklahoma shows significant lateral velocity variations implying that the crustal structure in the upper crust is more complex than an overall granitic basement may suggest. We observe a high velocity anomalies at 5 km depth (Figure 9a; regions A and B) in roughly NW-SE direction. This prominent high velocity region extends down to depths of ~15 km (Figure 9b, c; Region A) but decreases in intensity and lateral extent as the depth increases. Region A appears to be bounded at its eastern side by the Nemaha fault system. Cross-sections CC', DD' and EE' (Figure 10 c, d, e) show these high velocity anomalies in the upper crust as well. These high velocity anomalies correlate with the gravity anomalies. Chen (2016) interpreted this anomaly as an evidence for the extension of the Midcontinent Rift into northern Oklahoma. Our model extends deeper in this region and we observe that the velocity anomaly is only present in the upper-middle crust extending down to about 20 km in depth (Figure 9, Figure 10c). We correlate this high velocity anomaly with the occurrence of intra-basement reflectors in this region. Several authors (Chopra et al., 2018; Kolawole et al., 2020) have mapped these reflectors in 3-D (industry) active seismic data in depths between 8 to 10 km and have interpreted them as mafic sill intrusions (Kolawole et al., 2020). The mafic nature of these intra-basement reflectors may explain the anomalously high velocity observed in our model and would suggest mafic layering over a significant larger depth range, as the industry-scale active source are restricted in their depth extent.

We observe another high velocity anomaly in south-central Oklahoma (Figure 9 a, b, c, d; Region B) which appears more complex. We observe a decreasing intensity in the southern part with depth while the anomaly in the northern seems to be stronger in the

middle crust. The southern anomaly corresponds to a magnetic high (Figure 10f) while the northern anomaly corresponds to a magnetic low. The different magnetic signatures of the two anomalies indicate differences in lithological composition of the shallow to mid

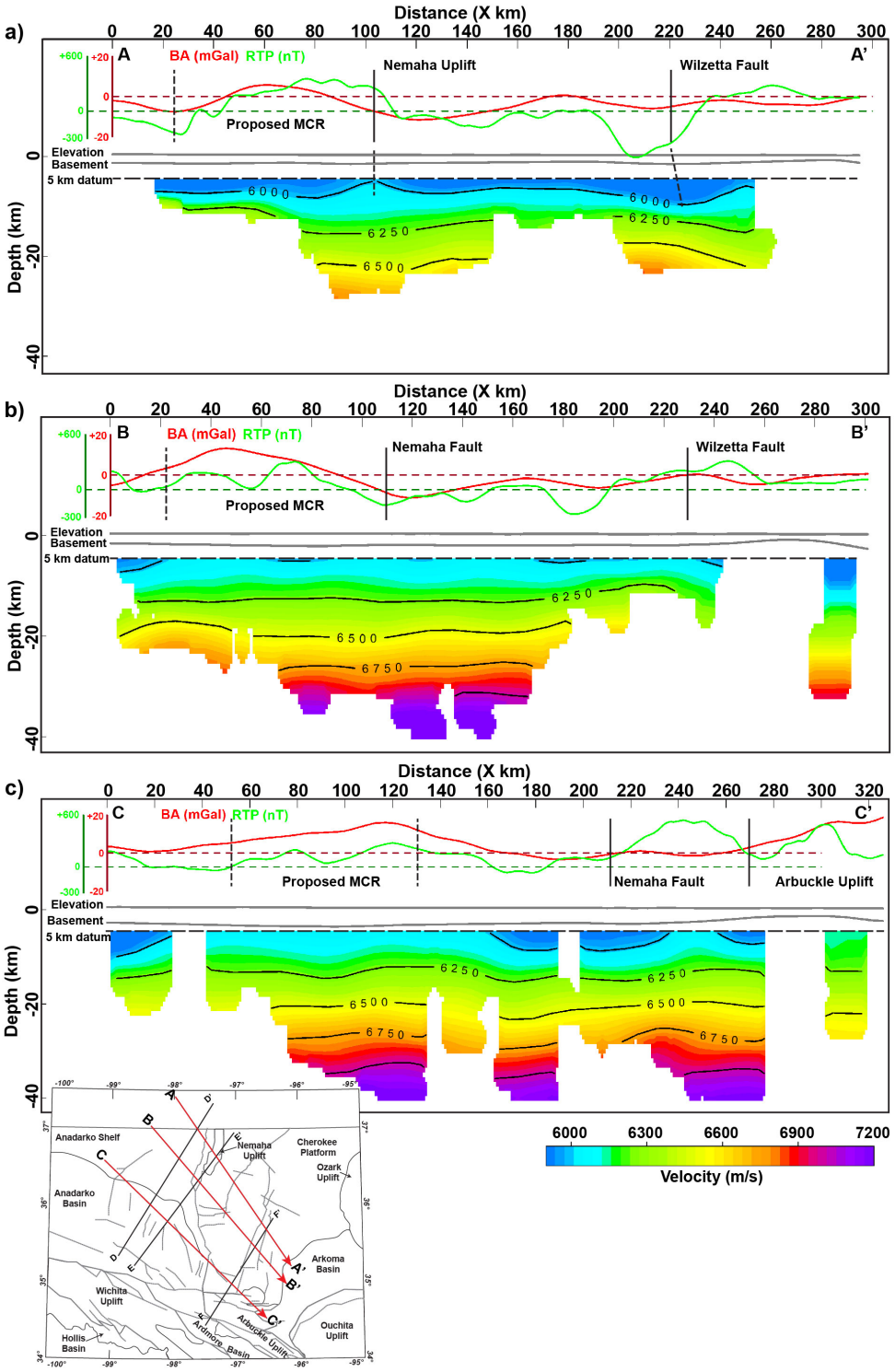

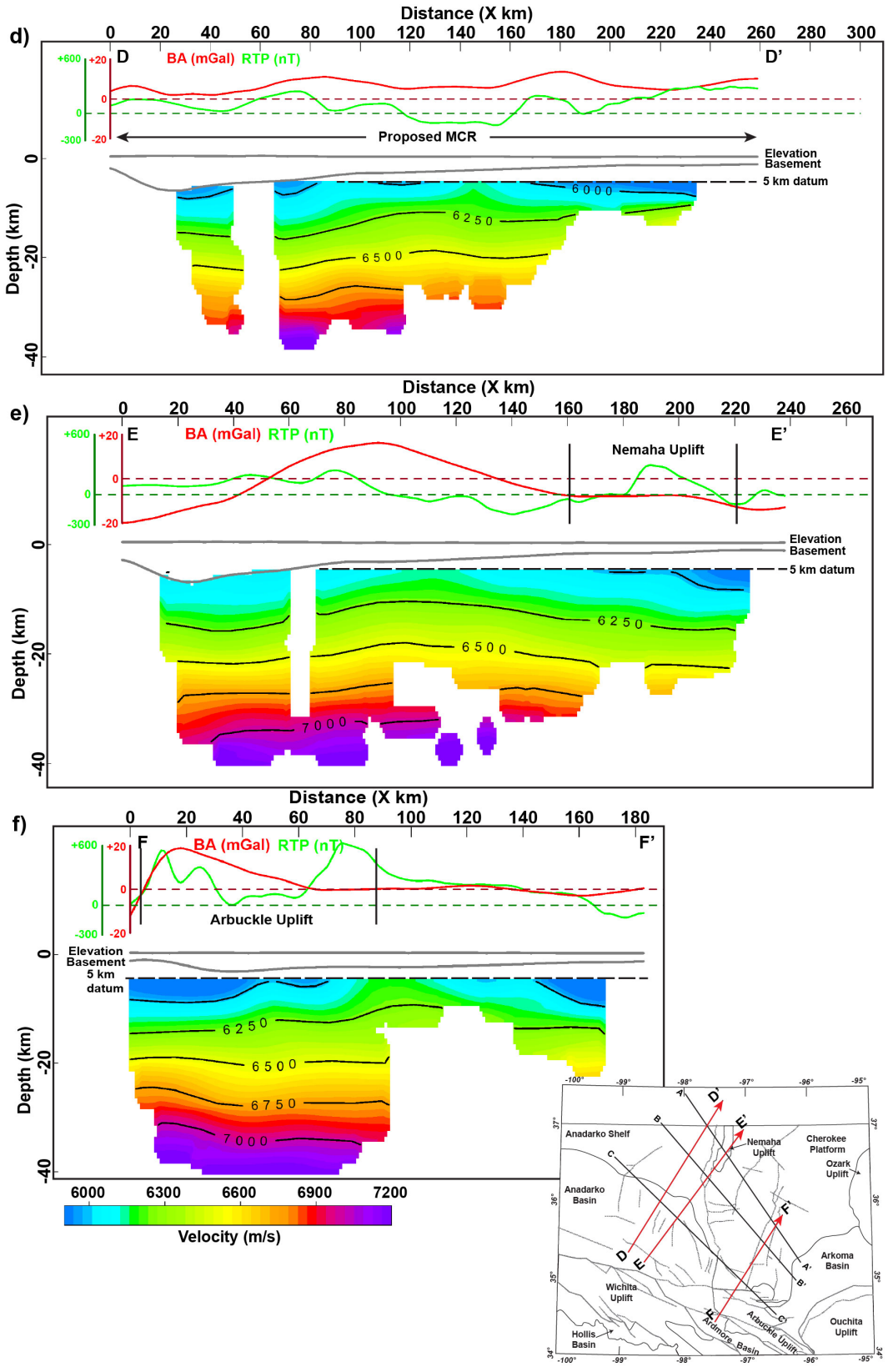

Figure 10. Pg-velocity model cross-sections. "Proposed MCR" indicates the tentative continuation of the Midcontinent Rift as suggested by previous studies. See text for discussion.

crust. The magnetic high on the southern side (Figure 10f) is close to the Arbuckle uplift, which could indicate that this magnetic anomaly is related to the deformation of the crustal rocks during the uplift. However, we also note is that this area has larger cell size and comparatively lower number of rays (Figure 5). Subsequently, the velocities here are less well constrained compared to other parts in our model. The high velocity anomaly on the northern side in the middle crust is overlain by a low velocity anomaly in the upper crust (Figure 10a), which can explain the absence of a gravity anomaly that would be expected with an isolated high or low velocity anomaly. As gravity data represent the integrated crustal structure in the subsurface, the combination of this low and high velocity anomaly may lead to an absence of a pronounced gravity anomaly.

We observe lower velocities in the north-east corner (Figure 9b-e; region C) in the velocity-depth cross-sections up to depths of ~25 km. These low velocity anomalies can be correlated with the Nemaha uplift in this area. The low velocity anomaly seems to extend deeper than 25 km into the lower crust (Figure 9f) but due to lack of data coverage in region C deeper than 30 km, it is difficult to estimate the depth extent of this anomaly. AA' and EE' (Figure 10) show a decrease in mid-crustal P-wave velocity associated with the Nemaha uplift and northern part of the Nehama fault system in cross sections that run both across and along this fault zone. The lower velocities are observed up to 25 – 30 km depth, which suggests that the Nemaha fault zone has a deep root in the crust. The Wilzetta fault zone is also observed as a low velocity anomaly in the upper crust in the AA' cross-section. The Anadarko basin region in the west is represented with generally lower velocities in the upper, mid, and lower crust (Figure 9).

P-wave velocities in the lower crust range from 7-7.3 km/s which are higher than the global average for shields and platform tectonic regime (Christensen & Mooney, 1995). Our velocity model therefore is in agreement with the assumption of a mafic lower crust in Oklahoma, as suggested by several crustal evolution models. High lower crustal velocities were also observed in the vintage 2-D active seismic survey in Oklahoma (Brewer & Oliver, 1980; Buckey, 2012; Mitchell & Landisman, 1970; Tryggvason & Qualls, 1967). The presence of a high velocity lower crust throughout Oklahoma provides a strong evidence for the formation of granite-rhyolite province through crustal melting of older crust. Velocities in the lower crust as seen in BB', DD' and EE' (Figure 10) are mostly homogeneous and do not show significant lateral variations. We do not observe variation across the "Nd-line" in Oklahoma either. The "Nd-line" is regarded as a "suture-zone" based on

model age studies of the mid-continent's basement rocks (Nelson & DePaolo, 1985). Lack of velocity variations across the assumed suture zone does not confirm or deny its existence, as episodic accretion could have created a more complex terrain with the possibility of several sutures over time. Also, a variation in age does not necessarily imply a strong variation of velocity.

4.3 Implications on the Midcontinent Rift (MCR) Structure

The MCR, which is extended to central Kansas by most authors (Cannon & Hinze, 1992; Van Schmus & Hinze, 1985; Woelk & Hinze, 1991) (Figure 1), has a thick igneous crust formed as a result of syn-rift and post-rift igneous fill followed by basin inversion which thickened the crust further (C. A. Stein et al., 2015). The rift was formed about 1.1 Ga through extensional tectonics related to the collision of Laurentia and Amazonia and volcanism that is attributed to the presence of the mantle plume in the lithosphere (Van Schmus & Hinze, 1985; Vervoort & Green, 1997). The rift underwent compressive inversion which led to the thickening of the crust (C. A. Stein et al., 2015). In general, rifts are associated with low gravity anomalies due to the accommodation space created by the rift being filled by sedimentary rocks which have lower densities (C. A. Stein et al., 2015; S. Stein et al., 2018). The MCR is very unique in that the rift is filled with voluminous basalts and volcanic sequences that give it the characteristic strong positive gravity anomalies.

There is no clear evidence for surface and/or subsurface structural expression of the MCR in Oklahoma so far. Positive gravity anomalies in northern Oklahoma (Figure 1) have been used to postulate the existence of the MCR in Oklahoma (Kolawole et al., 2020; C. A. Stein et al., 2014) but the actual magnitudes of these anomalies are smaller by factors of 3 to 15 compared to the MCR in Kansas and Minnesota. Our model shows that positive but still moderate velocity anomalies can be associated with the gravity highs in the upper crust (~5-20 km). As discussed before, these anomalies are interpreted as intrusive sills in the basement. These high-velocity anomalies do not extend deeper which questions the presence of a rift structure in northern Oklahoma. Cross section CC' (Figure 10) show velocity variations across the proposed MCR. The high Vp anomaly associated with the gravity high is more prominent in the upper crust-middle crust in this cross-section. EE' cross-section cuts through the same gravity high as CC' but in an orientation parallel to the proposed rift structure (Figure 10). It is more evident in the profile EE' that

the velocity anomaly associated with the gravity high is related to the structure of the upper crust. DD' cross-section runs along the longitudinal axis of the proposed MCR. The lateral variation in P-wave velocity in the upper crust (lower velocities in the south and comparatively high velocities in the north) can also be correlated with the basement below the Anadarko basin structure which exhibits overall lower crustal velocities.

The geology of the mid-continent region has been influenced by several tectonic events, starting from the episodic emplacement of the granite-rhyolite province from 1.5-1.3 Ga, followed by midcontinent rifting event 1.1 Ga, Grenville orogeny (1.3-1.09 Ga) which led to the final assembly of Rodinia, followed by the intermittent breakup of Rodinia which lasted from 0.78-0.53 Ga, and finally led to the formation of the Southern Oklahoma Aulacogen. Mafic intrusions in the crust upper-middle crust which are related to the high velocity anomaly are present not only in the proposed MCR region but are also observed in several active seismic studies in Oklahoma and elsewhere in the granite-rhyolite terrain in the Southern Oklahoma Aulacogen, Osage county, and northwest Texas (Buckey, 2012; Brewer et al., 1981, 1983, 1984; Elebiju et al., 2011; Mitchell & Landisman, 1970; McBride et al., 2018). We also interpret similar intrusive structures in the "Region B" in our velocity model as high velocity anomaly. The widespread presence of such structures across the southern granite-rhyolite terrain, suggests that the intrusions could be a result of a large-scale tectonic episode, and not necessarily related to the MCR.

4.4 Seismic Velocities and Spatial Distribution of Seismicity

The spatio-temporal distribution of seismicity in the investigated area is related to factors such as the presence of injection wells, injection volume, optimal fault orientations, porosity and permeability, and basement rock lithology (Ellsworth, 2013; Keranen et al., 2014; Qin et al., 2018, 2019). Many of the earthquakes in Oklahoma have occurred on previously unmapped faults, thus a lack of mapped faults cannot be used to argue for the lack of seismicity in this area. Figure 11 illustrates the location of earthquakes, injection wells, and injection volumes in the area. We have considered only the wells classified as salt-water disposal wells for this analysis, as the seismicity in Oklahoma has been connected to the waste water injection wells (Keranen et al., 2014). We observe a pronounced lack of seismicity in the high-velocity region A (Figure 11). In this area, the number of injection wells is still significant, and the injection volumes are similar to areas with high seismicity. We therefore argue that the lack of earthquakes in this area is related to the

variable basement lithology as indicated by the velocity distribution. Lithologic control on seismicity is observed in eastern Oklahoma, where high-volume injection wells have not caused an increase in seismicity (Shah & Keller, 2017). We suggest that the rocks associated with the high velocity anomalies are likely to have higher rock strength and thus would require higher stress conditions for fault rupture, and /or this basement region hosts less faults. This high velocity anomaly in shallow depths might be minimally fractured as compared to surrounding regions. Minimal fracturing would also imply low permeability and less vertical fluid migration, which would eventually lead to comparably low pore pressure buildup in the region. Basement lithology can influence the pore space availability, permeability and deformation capability, all of which in turn could control seismicity. As discussed above, deeper velocity anomalies in this region are also related to mafic intrusions at larger depths, and the anomaly is further confined by the Nemaha fault system to the east, as are the earthquake locations. We argue that all these observations suggest that the Nehama fault system is a deep-rooted crustal boundary with separates two crustal domains of different origin.

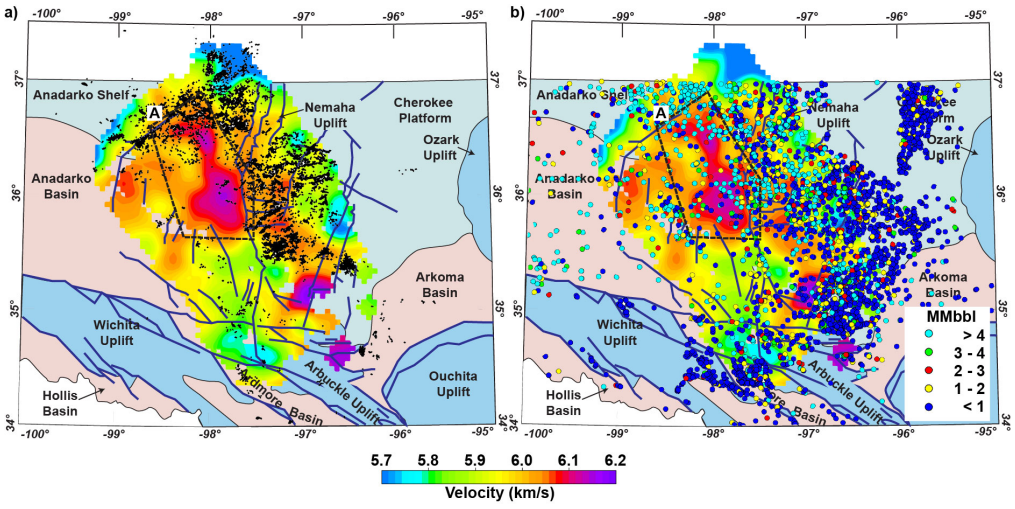

Figure 11. a) Earthquake locations; b) Total injection volume (MMbbl) for saltwater disposal wells from 2011-2017, overlain on 5 km velocity-depth slice.

5 Conclusions

In this study, common-mid-point sorting, stacking, and inversion techniques are applied to local earthquake waveform data in the central part of the mid-continent. In con-

trast to traditional local earthquake tomography (LET) studies from Oklahoma that have imaged the upper crust, our methodology results in a 3-D velocity model for significantly larger depths. Our results suggest a more heterogeneous upper and middle crust and a relatively homogeneous lower crust. These observations are interpreted to reflect a complex geologic history including deformations in the upper and mid-crustal depths and a possible homogenization of the lower crust through melting. The high velocity (>7 km/s) lower crust is indicative of mafic composition. This provides strong evidence for the evolution of the Granite-Rhyolite province from basaltic underplating and crustal melting. Structural evidence for a deep Midcontinent rift structure is not observed in Oklahoma. Several (possibly mafic) intrusions are interpreted in the upper-middle crust from high velocity anomalies which have previously been associated to the MCR extension in Oklahoma. However, the widespread occurrence of these intrusions in Oklahoma may suggest their derivation from a regional tectonic event as opposed to more local MCR event in Oklahoma. We interpret the Nemaha fault system as a deep-seated discontinuity which separates two crustal domains of different origin. Our results also suggest a lithologic control on induced seismicity in Oklahoma.

The suggested workflow is potentially applicable to other areas with similar datasets. Robust 3-D velocity models derived by this methodology can also be used for improved earthquake localization, and as initial models for local high-resolution LET analysis.

Acknowledgments

Waveform data used in this study can be downloaded from Incorporated Research Institutions for Seismology Data Management Center (IRIS-DMC, `https://ds.iris.edu/ds/nodes/dmc/data/#access`). Earthquake catalog for Oklahoma can be accessed through Oklahoma Geological Survey at `http://www.ou.edu/ogs/research/earthquakes/catalogs`. We would like to thank Dr. Brett Carpenter and Dr. Xiaowei Chen for thoughtful discussions that greatly improved our manuscript. We would also like to thank Dr. Jefferson Chang for providing the HypoDD relocated catalog used in this study.

References

Agena, W. F., Lee, M. W., & Grow, J. A. (1989). *Reprocessing of the COCORP data recorded across the Wichita Mountain uplift and the Anadarko basin in southern Oklahoma* (Tech. Rep.).

Amato, J. M., Heizler, M. T., Boullion, A. O., Sanders, A. E., Toro, J., McLemore, V. T., & Andronicos, C. L. (2011). Syntectonic 1.46 Ga magmatism and rapid cooling of a gneiss dome in the southern Mazatzal Province: Burro Mountains, New Mexico. *Geological Society of America Bulletin*, *123*(9-10), 1720–1744. doi: 10.1130/B30337.1

Anderson, J., & Bender, E. (1989). Nature and origin of Proterozoic A-type granitic magmatism in the southwestern United States of America. *Lithos*, *23*(1-2), 19–52. doi: 10.1016/0024-4937(89)90021-2

Astiz, L., Earle, P., & Shearer, P. (1996). Global Stacking of Broadband Seismograms. *Seismological Research Letters*, *67*(4), 8–18. doi: 10.1785/gssrl.67.4.8

Behm, M. (2009). 3-D modelling of the crustal S -wave velocity structure from active source data: application to the Eastern Alps and the Bohemian Massif. *Geophysical Journal International*, *179*(1), 265–278. doi: 10.1111/j.1365-246X.2009.04259.x

Behm, M., Brückl, E., Chwatal, W., & Thybo, H. (2007). Application of stacking and inversion techniques to three-dimensional wide-angle reflection and refraction seismic data of the Eastern Alps. *Geophysical Journal International*, *170*(1), 275–298. doi: 10.1111/j.1365-246X.2007.03393.x

Bickford, M. E., Harrower, K. L., Hoppe, W. J., Nelson, B. K., Nusbaum, R. L., & Thomas, J. J. (1981). Rb-Sr and U-Pb geochronology and distribution of rock types in the Precambrian basement of Missouri and Kansas. *Geological Society of America Bulletin*, *92*, 323–341. doi: 10.1130/0016-7606(1981)92<323:RAUGAD>2.0.CO;2

Bickford, M. E., & Lewis, R. D. (1979). U-Pb geochronology of exposed basement rocks in Oklahoma. *Geological Society of America Bulletin*, *90*(6), 540. doi: 10.1130/0016-7606(1979)90<540:UGOEBR>2.0.CO;2

Bickford, M. E., Van Schmus, W., Karlstrom, K., Mueller, P., & Kamenov, G. (2015). Mesoproterozoic-trans-Laurentian magmatism: A synthesis of continent-wide age distributions, new SIMS U–Pb ages, zircon saturation temperatures, and Hf and Nd isotopic compositions. *Precambrian Research*, *265*, 286–312. doi: 10.1016/j.precamres.2014.11.024

Bickford, M. E., Van Schmus, W. R., & Zietz, I. (1986). Proterozoic history of the midcontinent region of North America. *Geology*, *14*(6), 492. doi: 10.1130/0091-7613(1986)14<492:PHOTMR>2.0.CO;2

Braeuer, B., Asch, G., Hofstetter, R., Haberland, C., Jaser, D., El-Kelani, R., & Weber, M.

(2012). High-resolution local earthquake tomography of the southern Dead Sea area. *Geophysical Journal International*, *191*(3), 881-897. doi: 10.1111/j.1365-246X.2012.05668.x

Brewer, J. A., Brown, L. D., Steiner, D., Oliver, J. E., Kaufman, S., & Denison, R. E. (1981). Proterozoic basin in the southern Midcontinent of the United States revealed by COCORP deep seismic reflection profiling. *Geology*, *9*(12), 569. doi: 10.1130/0091-7613(1981)9<569:PBITSM>2.0.CO;2

Brewer, J. A., Good, R., Oliver, J. E., Brown, L. D., & Kaufman, S. (1983). COCORP profiling across the Southern Oklahoma aulacogen: Overthrusting of the Wichita Mountains and compression within the Anadarko Basin. *Geology*, *11*(2), 109. doi: 10.1130/0091-7613(1983)11<109:CPATSO>2.0.CO;2

Brewer, J. A., Good, R., Oliver, J. E., Brown, L. D., & Kaufman, S. (1984). COCORP deep seismic reflection traverse across the southern Oklahoma Aulacogen. *Technical Proceedings of the 1981 AAPG Mid-Continent Regional Meeting, 1984*, 191–194.

Brewer, J. A., & Oliver, J. E. (1980). Seismic reflection studies of deep crustal structure. *Annual Review of Earth and Planetary Sciences*, *8*(205-230).

Buckey, A. (2012). An integrated geophysical analysis of crustal structure in the Wichita Uplift region of southern Oklahoma. *The Shale Shaker*, *62*(6), 432–452.

Buehler, J. S., & Shearer, P. M. (2013). Sn propagation in the Western United States from common midpoint stacks of USArray data. *Geophysical Research Letters*, *40*(23), 6106–6111. doi: 10.1002/2013GL057680

Campbell, J. A. (2007). Understanding the structure of the Wichita uplift, southern Oklahoma. *Shale Shaker*, *1918*(December), 87–97.

Campbell, J. A., & Weber, J. L. (2006). Wells drilled to basement to basement in Oklahoma. *Oklahoma Geological Survey Special Publication 2006-1*.

Cannon, W. F., & Hinze, W. J. (1992). Speculations on the origin of the North American Midcontinent rift. *Tectonophysics*, *213*(1-2), 49–55. doi: 10.1016/0040-1951(92)90251-Z

Chen, C. (2016). *Comprehensive analysis of Oklahoma earthquakes: from earthquake monitoring to 3D tomography and relocation* (Unpublished doctoral dissertation). University of Oklahoma.

Chichester, B., Rychert, C., Harmon, N., Lee, S., Frederiksen, A., & Zhang, H. (2018). Seismic Imaging of the North American Midcontinent Rift Using S -to- P Receiver

Functions. *Journal of Geophysical Research: Solid Earth*, *123*(9), 7791–7805. doi: 10.1029/2018JB015771

Chopra, S., Marfurt, K. J., Kolawole, F., & Carpenter, B. M. (2018). Nemaha Strike-Slip Fault Expression on 3-D Seismic Data in SCOOP Trend. *AAPG Explorer*(June), 18–19.

Christensen, N. I., & Mooney, W. D. (1995). Seismic velocity structure and composition of the continental crust: A global view. *Journal of Geophysical Research*, *100*(B6), 9761–9788. doi: 10.1029/95JB00259

Darold, A. P., Holland, A. A., Jennifer, K., & Gibson, A. R. (2015). *Oklahoma Earthquake Summary Report 2014* (Tech. Rep.).

Denison, R. E., Lidiak, E. G., Bickford, M. E., & Kisvarsanyi, E. B. (1984). Geology and geochronology of Precambrian rocks in the Central Interior region of the United States. *US Geological Survey Professional Paper*, *1241 C*, 1–13. doi: 10.3133/pp1241c

Elebiju, O. O., Matson, S., Randy Keller, G., & Marfurt, K. J. (2011). Integrated geophysical studies of the basement structures, the Mississippi chert, and the Arbuckle Group of Osage County region, Oklahoma. *AAPG Bulletin*, *95*(3), 371–393. doi: 10.1306/08241009154

Ellsworth, W. L. (2013). Injection-Induced Earthquakes. *Science*, *341*(6142), 1225942–1225942. doi: 10.1126/science.1225942

Evanzia, D., Pulliam, J., Ainsworth, R., Gurrola, H., & Pratt, K. (2014). Seismic Vp & Vs tomography of Texas & Oklahoma with a focus on the Gulf Coast margin. *Earth and Planetary Science Letters*, *402*(C), 148–156. doi: 10.1016/j.epsl.2013.12.027

Frost, C. D., & Frost, B. R. (2011). On Ferroan (A-type) Granitoids: their Compositional Variability and Modes of Origin. *Journal of Petrology*, *52*(1), 39–53. doi: 10.1093/petrology/egq070

Frost, C. D., & Frost, B. R. (2013). Proterozoic ferroan feldspathic magmatism. *Precambrian Research*, *228*, 151–163. doi: 10.1016/j.precamres.2013.01.016

Gajewski, D., & Pšenčik, I. (1987). Computation of high-frequency seismic wavefields in 3-D laterally inhomogeneous anisotropic media. *Geophysical Journal International*, *91*(2), 383–411. doi: 10.1111/j.1365-246X.1987.tb05234.x

Gajewski, D., & Pšenčík, I. (1989). Ray synthetic seismograms in 3-d laterally inhomogeneous anisotropic structures-program anray89. *LBL Center for Computational Seis-*

mology, Berkeley, CA.

Garner, D. L., & Turcotte, D. L. (1984). The thermal and mechanical evolution of the Anadarko basin. *Tectonophysics*, *107*(1-2), 1–24. doi: 10.1016/0040-1951(84)90026-X

Gilbert, M., Denison, R., Reed, J., Bickford, M., Houston, R., Link, P., . . . Van Schmus, W. (1993). Late proterozoic to early cambrian basement of oklahoma. *Reed JC, Bickford ME, Houston RS, and four others, eds., Precambrian: Conterminous US: Boulder, Colorado, Geological Society of America, The Geology of North America*, *2*, 303–314.

Goodge, J. W., & Vervoort, J. D. (2006). Origin of Mesoproterozoic A-type granites in Laurentia: Hf isotope evidence. *Earth and Planetary Science Letters*, *243*(3-4), 711–731. doi: 10.1016/j.epsl.2006.01.040

Hinze, W. J., Allen, D. J., Braile, L. W., & Mariano, J. (1997). The Midcontinent Rift System: A major Proterozoic continental rift. In *Middle proterozoic to cambrian rifting, central north america* (Vol. 312, pp. 7–35). Geological Society of America. doi: 10.1130/0-8137-2312-4.7

Johnson, K. (2008). Geologic History of Oklahoma. *Educational Publication*, *9*, 3–8.

Karlstrom, K. E., Whitmeyer, S. J., Dueker, K., Williams, M. L., Bowring, S. A., Levander, A. R., . . . Keller, G. R. (2005). Synthesis of results from the CD-ROM Experiment: 4-D image of the lithosphere beneath the Rocky Mountains and implications for understanding the evolution of continental lithosphere. In *Geophysical monograph series* (Vol. 154, pp. 421–441). doi: 10.1029/154GM31

Karlstrom, K. E., Åhäll, K.-I., Harlan, S. S., Williams, M. L., McLelland, J., & Geissman, J. W. (2001). Long-lived (1.8–1.0 ga) convergent orogen in southern laurentia, its extensions to australia and baltica, and implications for refining rodinia. *Precambrian Research*, *111*(1), 5 - 30. doi: https://doi.org/10.1016/S0301-9268(01)00154-1

Keller, G., Lidiak, E., Hinze, W., & Braile, L. (1983). The Role of Rifting in the Tectonic Development of the Midcontinent, U.S.A. In *Tectonophysics* (Vol. 94, pp. 391–412). doi: 10.1016/B978-0-444-42198-2.50028-6

Keranen, K. M., Weingarten, M., Abers, G. A., Bekins, B. A., & Ge, S. (2014). Sharp increase in central Oklahoma seismicity since 2008 induced by massive wastewater injection. *Science*, *345*(6195), 448–451. doi: 10.1126/science.1255802

Kissling, E., Ellsworth, W. L., Eberhart-Phillips, D., & Kradolfer, U. (1994). Initial refer-

751 ence models in local earthquake tomography. *Journal of Geophysical Research: Solid*
752 *Earth*, *99*(B10), 19635–19646. doi: 10.1029/93JB03138

753 Kolawole, F., Simpson Turko, M., & Carpenter, B. M. (2020). Basement-controlled defor-
754 mation of sedimentary sequences, Anadarko Shelf, Oklahoma. *Basin Research*(August
755 2019), bre.12433. doi: 10.1111/bre.12433

756 Lidiak, E. G. (1996). Geochemistry of subsurface Proterozoic rocks in the eastern Mid-
757 continent of the United States: Further evidence for a within-plate tectonic setting. In
758 *Basement and basins of eastern north america* (Vol. 308, pp. 45–66). Geological Soci-
759 ety of America. doi: 10.1130/0-8137-2308-6.45

760 Loidl, B., Behm, M., Thybo, H., & Stratford, W. (2014). Three-dimensional seismic model
761 of crustal structure in Southern Norway. *Geophysical Journal International*, *196*(3),
762 1643–1656. doi: 10.1093/gji/ggt471

763 Lynn, H. B., Hale, L. D., & Thompson, G. A. (1981). Seismic reflections from the basal con-
764 tacts of batholiths. *Journal of Geophysical Research: Solid Earth*, *86*(B11), 10633–
765 10638. doi: 10.1029/JB086iB11p10633

766 McBride, J. H., William Keach, R., Leetaru, H. E., & Smith, K. M. (2018). Visualizing
767 Precambrian basement tectonics beneath a carbon capture and storage site, Illinois
768 Basin. *Interpretation*, *6*(2), T257-T270. doi: 10.1190/INT-2017-0116.1

769 McGlannan, A. J., & Gilbert, H. (2016). Crustal signatures of the tectonic development of
770 the North American midcontinent. *Earth and Planetary Science Letters*, *433*, 339–
771 349. doi: 10.1016/j.epsl.2015.10.048

772 Mitchell, B., & Landisman, M. (1970). Interpretation of a crustal section across Oklahoma.
773 *Geological Society of America Bulletin*, *81*, 2647–2656.

774 Muehlberger, W. R., Denison, R. E., & Lidiak, E. G. (1967). Basement Rocks in Continental
775 Interior of United States. *AAPG Bulletin*, *51*(12), 2351–2380. doi: 10.1306/5D25C277
776 -16C1-11D7-8645000102C1865D

777 Muehlberger, W. R., Hedge, C. E., Denison, R. E., & Marvin, R. F. (1966). Geochronology
778 of the midcontinent region, United States: 3. Southern area. *Journal of Geophysical*
779 *Research*, *71*(22), 5409–5426. doi: 10.1029/JZ071i022p05409

780 Nelson, B. K., & DePaolo, D. J. (1985). Rapid production of continental crust 1.7 to 1.9 b.y.
781 ago: Nd isotopic evidence from the basement of the North American mid-continent.
782 *Geological Society of America Bulletin*, *96*(6), 746. doi: 10.1130/0016-7606(1985)
783 96<746:RPOCCT>2.0.CO;2

Northcutt, R. A., & Campbell, J. A. (1996). Geologic Provinces of Oklahoma. *Shale Shaker*. doi: 10.1306/7834D65C-1721-11D7-8645000102C1865D

Pei, S., Chen, Y. J., Feng, B., Gao, X., & Su, J. (2013). High-resolution seismic velocity structure and azimuthal anisotropy around the 2010 Ms=7.1 Yushu earthquake, Qinghai, China from 2D tomography. *Tectonophysics*, *584*, 144–151. doi: 10.1016/j.tecto.2012.08.020

Pei, S., Peng, Z., & Chen, X. (2018). Locations of Injection-Induced Earthquakes in Oklahoma Controlled by Crustal Structures. *Journal of Geophysical Research: Solid Earth*, *123*(3), 2332–2344. doi: 10.1002/2017JB014983

Phinney, R. A., & Jurdy, D. M. (1979). Seismic imaging of deep crust. *Geophysics*, *44*(10), 1637–1660. doi: 10.1190/1.1440927

Pratt, T. L., Hauser, E. C., & Nelson, K. D. (1992). Widespread buried precambrian layered sequences in the midcontinent- evidence for large proterozoic depositional basins. *AAPG Bulletin*, *76*(9), 1384–1401.

Qin, Y., Chen, X., Carpenter, B. M., & Kolawole, F. (2018). Coulomb Stress Transfer Influences Fault Reactivation in Areas of Wastewater Injection. *Geophysical Research Letters*, *45*(20), 059–11. doi: 10.1029/2018GL079713

Qin, Y., Chen, X., Walter, J. I., Haffener, J., Trugman, D. T., Carpenter, B. M., . . . Kolawole, F. (2019). Deciphering the Stress State of Seismogenic Faults in Oklahoma and Southern Kansas Based on an Improved Stress Map. *Journal of Geophysical Research: Solid Earth*, *124*(12), 12920–12934. doi: 10.1029/2019JB018377

Rawlinson, N., & Sambridge, M. (2003). Seismic traveltime tomography of the crust and lithosphere. In *Advances in geophysics* (Vol. 46, pp. 81–198). doi: 10.1016/S0065-2687(03)46002-0

Schoenball, M., & Ellsworth, W. L. (2017). Waveform-Relocated Earthquake Catalog for Oklahoma and Southern Kansas Illuminates the Regional Fault Network. *Seismological Research Letters*, *88*(5), 1252–1258. doi: 10.1785/0220170083

Shah, A. K., & Keller, G. R. (2017). Geologic influence on induced seismicity: Constraints from potential field data in Oklahoma. *Geophysical Research Letters*, *44*(1), 152–161. doi: 10.1002/2016GL071808

Shaw, C. A., Heizler, M. T., & Karlstrom, K. E. (2005). 40Ar/39Ar thermochronologic record of 1.45–1.35 Ga intracontinental tectonism in the southern Rocky Mountains: Interplay of conductive and advective heating with intracontinental deformation. In

Geophysical monograph series (Vol. 154, pp. 163–184). doi: 10.1029/154GM12

Shen, W., Ritzwoller, M. H., & Schulte-Pelkum, V. (2013). Crustal and uppermost mantle structure in the central U.S. encompassing the Midcontinent Rift. *Journal of Geophysical Research: Solid Earth*, *118*(8), 4325–4344. doi: 10.1002/jgrb.50321

Sims, P. K., Saltus, R. W., & Anderson, E. D. (2005). Structure Map of the Continental United States – An Interpretation of Geologic and Aeromagnetic Data of the Continental United States — an Interpretation of Geologic and Aeromagnetic Data. *U.S. Geological Survey Open-file report 2005-1029*, 29.

Slagstad, T., Culshaw, N. G., Daly, J. S., & Jamieson, R. A. (2009). Western Grenville Province holds key to midcontinental Granite-Rhyolite Province enigma. *Terra Nova*, *21*(3), 181–187. doi: 10.1111/j.1365-3121.2009.00871.x

Stein, C. A., Kley, J., Stein, S., Hindle, D., & Keller, G. R. (2015). North America's Midcontinent Rift: When rift met LIP. *Geosphere*, *11*(5), 1607–1616. doi: 10.1130/GES01183.1

Stein, C. A., Stein, S., Elling, R., Keller, G. R., & Kley, J. (2018). Is the "Grenville Front" in the central United States really the Midcontinent Rift? *GSA Today*, *28*(5), 4–10. doi: 10.1130/GSATG357A.1

Stein, C. A., Stein, S., Merino, M., Randy Keller, G., Flesch, L. M., & Jurdy, D. M. (2014). Was the Midcontinent Rift part of a successful seafloor-spreading episode? *Geophysical Research Letters*, *41*(5), 1465–1470. doi: 10.1002/2013GL059176

Stein, S., Stein, C. A., Elling, R., Kley, J., Keller, G. R., Wysession, M., . . . Moucha, R. (2018). Insights from north america's failed midcontinent rift into the evolution of continental rifts and passive continental margins. *Tectonophysics*, *744*, 403–421.

Tave, M. A. (2013). *Imaging of the crust and moho beneath oklahoma using receiver functions and pn tomography; with emphasis on the southern oklahoma aulacogen* (Unpublished doctoral dissertation).

Thomas, W. A. (1991). The appalachian-ouachita rifted margin of southeastern north america. *Geological Society of America Bulletin*, *103*(3), 415–431.

Thybo, H., & Artemieva, I. (2013). Moho and magmatic underplating in continental lithosphere. *Tectonophysics*, *609*, 605–619. doi: 10.1016/j.tecto.2013.05.032

Thybo, H., Sandrin, A., Nielsen, L., Lykke-Andersen, H., & Keller, G. (2006). Seismic velocity structure of a large mafic intrusion in the crust of central Denmark from project ESTRID. *Tectonophysics*, *420*(1-2), 105–122. doi: 10.1016/j.tecto.2006.01.029

Tong, P., Yang, D., Li, D., & Liu, Q. (2017). Time-evolving seismic tomography: The method and its application to the 1989 loma prieta and 2014 south napa earthquake area, california. *Geophysical Research Letters*, *44*(7), 3165–3175.

Toth, C. R. (2014). *Separation of the earthquake tomography inverse problem to refine hypocenter locations and tomographic models: A case study from central oklahoma* (Unpublished doctoral dissertation). University of Oklahoma.

Tryggvason, E., & Qualls, B. R. (1967). Seismic refraction measurements of crustal structure in Oklahoma. *Journal of Geophysical Research*, *72*(14), 3738–3740. doi: 10.1029/JZ072i014p03738

Van Schmus, W. R., Bickford, M. E., & Turek, A. (1996). Proterozoic geology of the east-central Midcontinent basement. In *Basement and basins of eastern north america* (Vol. 308, pp. 7–32). Geological Society of America. doi: 10.1130/0-8137-2308-6.7

Van Schmus, W. R., & Hinze, W. J. (1985). The Midcontinent Rift System. *Annual Review of Earth and Planetary Sciences*, *13*(1), 345–383. doi: 10.1146/annurev.ea.13.050185.002021

Vervoort, J. D., & Green, J. C. (1997). Origin of evolved magmas in the Midcontinent rift system, northeast Minnesota: Nd-isotope evidence for melting of Archean crust. *Canadian Journal of Earth Sciences*, *34*(4), 521–535. doi: 10.1139/e17-042

Whitmeyer, S. J., & Karlstrom, K. E. (2007). Tectonic model for the Proterozoic growth of North America. *Geosphere*, *3*(4), 220–259. doi: 10.1130/GES00055.1

Woelk, T. S., & Hinze, W. J. (1991). Model of the midcontinent rift system in northeastern Kansas. *Geology*, *19*(3), 277. doi: 10.1130/0091-7613(1991)019<0277:MOTMRS>2.3.CO;2

Zhang, H., Lee, S., Wolin, E., Bollmann, T. A., Revenaugh, J., Wiens, D. A., ... Jurdy, D. M. (2016). Distinct crustal structure of the North American Midcontinent Rift from P wave receiver functions. *Journal of Geophysical Research: Solid Earth*, *121*(11), 8136–8153. doi: 10.1002/2016JB013244

Zhu, X., & McMechan, G. A. (1989). 2-D tomographic imaging of velocities in the Wichita uplift-Anadarko basin region of southwestern Oklahoma. *Bulletin of the Seismological Society of America*, *79*(3), 873–887.